⌘ *Author's Choice*

THE JOURNAL OF BIOLOGICAL CHEMISTRY VOL. 285, NO. 21, pp. 16231–16238, May 21, 2010

Flightless-I (Fli-I) Regulates the Actin Assembly Activity of Diaphanous-related Formins (DRFs) Daam1 and mDia1 in Cooperation with Active Rho GTPase*[S]

Received for publication, October 26, 2009, and in revised form, February 9, 2010 Published, JBC Papers in Press, March 11, 2010, DOI 10.1074/jbc.M109.079236

Tomohito Higashi[‡§1,2], Tomoyuki Ikeda[‡1], Takaaki Murakami[‡], Ryutaro Shirakawa[‡¶2], Mitsunori Kawato[‡3], Katsuya Okawa[‖4], Mikio Furuse[§], Takeshi Kimura[‡], Toru Kita[‡5], and Hisanori Horiuchi[‡¶6]

From the [‡]Department of Cardiovascular Medicine, Graduate School of Medicine, Kyoto University, Kyoto 606-8507, the [§]Department of Cell Biology, Kobe University Graduate School of Medicine, Kobe 650-0017, the [‖]Frontier Technology Center, Graduate School of Medicine, Kyoto University, Kyoto 606-8501, and the [¶]Department of Molecular and Cellular Biology, Institute of Development, Aging and Cancer, Tohoku University, Sendai 980-8575, Japan

Eukaryotic cells dynamically reorganize the actin cytoskeleton to regulate various cellular activities, such as cell shape change, cell motility, cytokinesis, and vesicular transport. Diaphanous-related formins (DRFs), such as Daam1 and mDia1, play central roles in actin dynamics through assembling linear actin filaments. It has been reported that the GTP-bound active Rho binds directly to DRFs and partially unleashes the intramolecular autoinhibition of DRFs. However, whether proteins other than Rho involve the regulation of the actin assembly activity of DRFs has been unclear. Here, we show that Flightless-I (Fli-I), a gelsolin family protein essential for early development, binds directly to Daam1 and mDia1. Fli-I enhances the intrinsic actin assembly activity of Daam1 and mDia1 *in vitro* and is required for Daam1-induced actin assembly in living cells. Furthermore, Fli-I promotes the GTP-bound active Rho-mediated relief of the autoinhibition of Daam1 and mDia1. Thus, Fli-I is a novel positive regulator of Rho-induced linear actin assembly mediated by DRFs.

Formin proteins regulate the actin dynamics by assembling actin filaments through their formin homology-1 (FH1)[7] and formin homology-2 (FH2) domains (1–7). The FH2 domain nucleates the actin assembly and elongates the actin filament at the growing barbed end, supported by the FH1 domain, which recruits the globular actin complexed with profilin (8, 9). The actin assembly activity of a group of formins is under control of Rho family GTPases, and they are classified as diaphanous-related formins (DRFs) (10). Daam1 (Dishevelled associated activator of morphogenesis 1) and mDia1 (mammalian Diaphanous homolog 1, which is also known as DIA1, DIAP1, DFNA1, and DRF1) are members of the DRFs (10). These two proteins have similar domain structures (Fig. 1*A*). The amino-terminal diaphanous inhibitory domain (DID) and the carboxyl-terminal diaphanous autoinhibitory domain (DAD) segment form an intramolecular interaction to restrain the actin assembly activity of FH1-FH2 domains (11–14). The binding of GTP-Rho to the GTPase-binding domain (GBD) has been demonstrated to unleash the autoinhibitory interaction, although the stimulatory effect of GTP-Rho on the actin assembly activity *in vitro* was incomplete (12, 15). Thus, it has been proposed that a more complicated mechanism regulates the actin assembly activity of DRFs. To further clarify the regulatory mechanism of DRF, we attempted to isolate a DRF-binding protein by affinity chromatography using recombinant carboxyl-terminal protein fragment of Daam1.

EXPERIMENTAL PROCEDURES

Constructs, Recombinant Proteins, Antibodies, and Other Materials—The preparation of cDNAs encoding human Daam1 fragments (Daam1 NT, amino acids (aa) 41–477; Daam1 CT, aa 490–1078; and Daam1 CT F1046A), human mDia1 fragments (mDia1 NT, aa 69–450; mDia1 CT, aa 492–1263; and mDia1 CT F1203A) (Fig. 1, *A* and *B*), and human RhoA were described before (11). cDNAs encoding Daam1 DAD (aa 992–1078), mDia1 DAD (aa 1145–1263), Daam1 CT L1040A, and mDia1 CT L1197A were produced by PCR using their respective CT fragments as templates. The cDNA encoding human Flightless-I (Fli-I) was obtained by PCR using Marathon-Ready human bone marrow cDNA (Clontech) as a tem-

* This work was supported in part by the Ministry of Education, Culture, Sports, Science, and Technology of Japan Research Grant 20013201 (to H. H.), the Takeda Science Foundation (to H. H.), Novartis Foundation (Japan) for the Promotion of Science (to H. H.), and Global COE Program "Center for Frontier Medicine" from the Ministry of Education, Culture, Sports, Science and Technology, Japan.

⌘ *Author's Choice*—Final version full access.

[S] The on-line version of this article (available at http://www.jbc.org) contains supplemental Figs. 1 and 2.

[1] Both authors contributed equally to this work.

[2] Supported by the Japan Society for the Promotion of Science Research Fellowship for Young Scientists.

[3] Present address: Dept. of Cardiology, Nishi-Kobe Medical Center, Kobe 651-2273, Japan.

[4] Present address: Drug Discovery Research Laboratories, Kyowa Hakko Kirin Co. Ltd., Shizuoka 411-8731, Japan.

[5] Present address: Kobe City Medical Center General Hospital, Kobe 650-0046, Japan.

[6] To whom correspondence should be addressed. Tel. and Fax: 81-22-717-8463; E-mail: horiuchi@idac.tohoku.ac.jp.

[7] The abbreviations used are: FH1, formin homology 1; FH2, formin homology 2; DRF, diaphanous-related formin; DID, diaphanous inhibitory domain; DAD, diaphanous autoinhibitory domain; GBD, GTPase binding domain; LRR, leucine-rich repeat; Gsn, gelsolin; GST, glutathione *S*-transferase; mAb, monoclonal antibody; MALDI-TOF, matrix-assisted laser desorption ionization time-of-flight; aa, amino acid; siRNA, small interfering RNA; GFP, green fluorescent protein; WT, wild type; GppNHp, guanosine 5′-[β,γ-imido]trisphosphate; CT, carboxyl-terminal fragment; NT, amino-terminal fragment; PCP, planar cell polarity.

plate. The cDNAs encoding Fli-I fragments (LRR, aa 1–460; G1–3, aa 461–869; G4–6, aa 869–1269; and G1–6, aa 461–1269) (Fig. 2*C*) were obtained by PCR using full-length Fli-I as a template. For knockdown studies, two different siRNAs against mouse Fli-I (#159473 and #76439, designated as #1 and #2, respectively) and control siRNA were provided by Ambion. Full-length Fli-I, which is insensitive to siRNA against mouse Fli-I, was produced by PCR using human Fli-I as a template. Nucleotide substitutions that do not change the amino acid sequence were introduced at the #1 and #2 siRNA target sites, respectively. The cDNAs encoding human cytosolic gelsolin (Gsn) fragments (G1–3, aa 1–357; G4–6, aa 358–730) were obtained by PCR using Marathon-Ready human bone marrow cDNA (Clontech) as a template. All the sequences of the PCR products were confirmed by DNA sequencing. For expression in mammalian cells, Daam1 CT fragments were subcloned into pEGFP-C1 (Clontech). For generation of glutathione *S*-transferase (GST)-fused proteins, gene fragments were subcloned into pGEX-2T (GE Healthcare). For generation of His_6-tagged proteins, Daam1 NT, Daam1 CT, mDia1 NT, and mDia1 CT were subcloned into pDEST17 (Invitrogen), and Fli-I and Gsn fragments were subcloned into pRSET1A (Invitrogen).

Recombinant proteins of Daam1 CT and mDia1 CT were expressed in *Escherichia coli* strain Rosetta (DE3) (Novagen), and the other proteins were expressed in *E. coli* strain BL21 (DE3) (Novagen). The proteins were purified with glutathione-Sepharose (GE Healthcare) for GST-fused proteins or with Ni^{2+}-nitrilotriacetic acid-agarose (Qiagen) for His_6-tagged proteins according to the manufacturers' instructions. His_6-Fli-I was further purified by Mono S cation exchange column (GE Healthcare) chromatography equilibrated with buffer A (50 mM Hepes/KOH (pH 7.4), 78 mM KCl, 4 mM $MgCl_2$, 2 mM EGTA, 0.2 mM $CaCl_2$, and 1 mM dithiothreitol). The preparation of GppNHp (a nonhydrolyzable GTP analog)- or GDP-bound form of RhoA was described previously (16). Purified proteins were dialyzed against buffer A, stored at 4 °C, and used within 14 days after dialysis. The protein concentrations were determined by the Bradford method (Bio-Rad) or from the intensity of protein bands of Coomassie Brilliant Blue-stained SDS-polyacrylamide gel using bovine serum albumin as a standard. Reagents used in this study were purchased from Sigma unless otherwise specified.

Anti-Fli-I rabbit polyclonal antibody used for immunodepletion was obtained by immunizing a rabbit with Fli-I G1–6. Anti-Fli-I (116.40) mouse monoclonal antibody (mAb) used for immunoblotting was purchased from Santa Cruz Biotechnology. Anti-actin (Ab-5), anti-His_6 (HIS-1), anti-GFP (7.1 and 13.1), and anti-tubulin (DM-14) mouse mAbs used for immunoblotting were from BD Transduction Laboratories, Sigma, Roche Applied Science, and Seikagaku Corp., respectively. Anti-hemagglutinin (3F10) rat mAb used for immunoblotting was from Roche Applied Science. Horseradish peroxidase-linked anti-rabbit IgG donkey polyclonal antibody (GE Healthcare) and anti-mouse IgG sheep polyclonal antibody (GE Healthcare) were used as secondary antibodies in the immunoblot analysis visualized by enhanced chemiluminescence method (GE Healthcare). Alexa-546-conjugated phalloidin used for fluorescence microscopy was from Invitrogen.

Affinity Chromatography of Platelet Cytosol Using Daam1 CT—A platelet pellet (10 g) was sonicated in buffer A containing protease inhibitor mixture (Sigma). After extensive dialysis against buffer A, the solution was ultracentrifuged at 100,000 × *g* for 1 h. The supernatant was filtrated twice with a 0.45-μm disc filter (Millipore) and used as platelet cytosol. Glutathione-Sepharose coated with 200 μg of GST-Daam1 CT WT or L1040A was incubated with 20 ml of platelet cytosol (4 mg of proteins/ml) for 2 h at 4 °C and washed five times with buffer A. Bead-associated proteins were eluted with Laemmli SDS sample buffer (17) and were analyzed by SDS-PAGE. Protein bands were excised from the Coomassie Brilliant Blue-stained gel and analyzed by MALDI-TOF mass spectrometry as described previously (11, 18).

Actin Assembly Assays—The pyrene-actin assembly assay was performed as described previously (7). In brief, purified and gel-filtrated actin (5% pyrene-labeled, 2 μM) was assembled in the presence of the indicated proteins, and the fluorescence intensity was monitored. The cytoplasmic actin assembly assay was also described previously (11). Briefly, glutathione-Sepharose coated with GST fusion protein was incubated at 37 °C for 10 min with platelet cytosol and ATP in the absence or presence of purified Fli-I. The beads were washed and fixed with 4% formaldehyde at 4 °C for 5 min, and the assembled actin on the beads was stained with rhodamine-phalloidin (Invitrogen). The fluorescence intensity of the beads was measured using an Arvo SX 1420 multilabel counter (PerkinElmer Life Sciences).

In Vitro Binding Assay—Glutathione beads coated with GST fusion protein were incubated with His_6-tagged protein(s) in buffer A containing 4% bovine serum albumin for 2 h at 4 °C. Beads were washed five times with buffer A, and bead-associated proteins were analyzed by immunoblot using anti-His_6 antibody.

Immunodepletion of Fli-I from the Platelet Cytosol—Protein A-agarose (Roche Applied Science) beads were incubated at 4 °C for 1 h with anti-Fli-I rabbit antiserum or preimmune serum and washed three times with phosphate-buffered saline. The beads were then incubated with 500 μl of platelet cytosol at 4 °C for 2 h and removed by centrifugation. The supernatant was incubated twice with antibody-bound beads. The resultant Fli-I-depleted cytosol and preimmune IgG-treated cytosol were examined by immunoblot analysis using anti-Fli-I mouse mAb and used for the cytoplasmic actin assembly assay.

Cell Culture and Staining—NIH 3T3 cells were cultured in Dulbecco's modified Eagle's medium supplemented with 10% fetal calf serum. For observation of Daam1 CT-induced stress fibers, cells were seeded at the density of 3.0×10^4 cells/ml on the coverslips. After 2 days, cells were transfected with pEGFP-C1 Daam1 CT WT, pEGFP-C1 Daam1 CT L1040A, or pEGFP vectors using Lipofectamine LTX (Invitrogen) with Plus reagent (Invitrogen) according to the manufacturer's instruction. Cells were cultured for 20 h in the low serum medium containing 0.5% fetal calf serum. The cells were then fixed with 1% formaldehyde in phosphate-buffered saline for 10 min, permeabilized with phosphate-buffered saline containing 0.2% Triton X-100 for 5 min, and stained with Alexa-568-conjugated phalloidin in phosphate-buffered saline containing 0.2% bovine serum albumin. Alternatively, cells were lysed with Laemmli SDS sample buffer (17) and analyzed by SDS-PAGE followed by immunoblotting. For

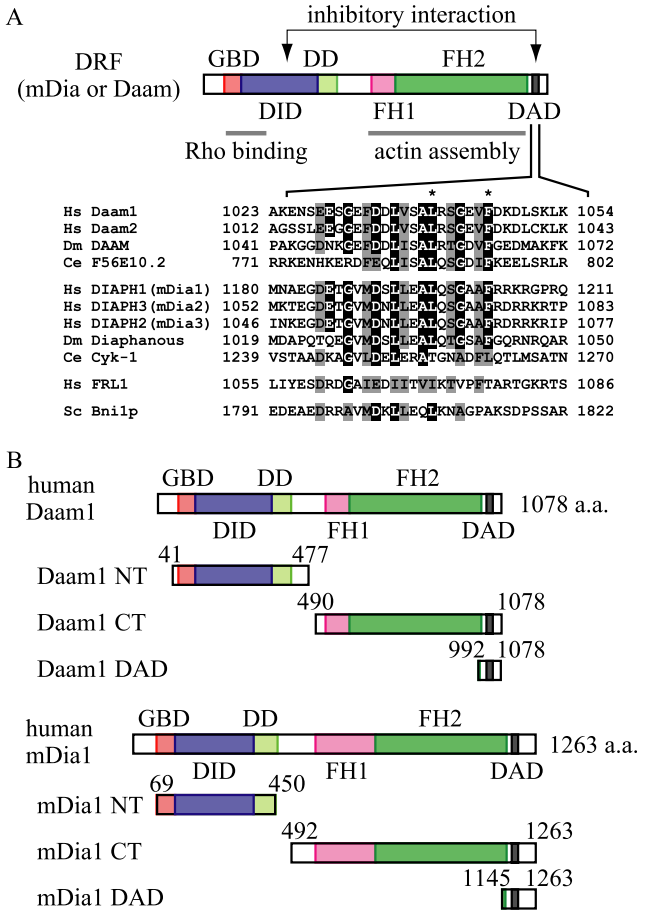

FIGURE 1. **DAD segment enhances the actin assembly activity of Daam1 CT in cytoplasmic environment.** *A* and *B*, domain structures of typical DRF (*A*) and Daam1 and mDia1 (*B*). The amino acid sequences of several DRF DAD segments are shown. *GBD*, GTPase-binding domain; *DD*, dimerization domain; *Hs, Homo sapiens*; *Dm, Drosophila melanogaster*; *Ce, Caenorhabditis elegans*; *Sc, Saccharomyces cerevisiae*. *Asterisks* in *A* show the mutated residues. *C* and *D*, cytoplasmic actin assembly assay (*C*) and pyrene actin assembly assay (*D*) of Daam1 CT mutants. The data shown in *C* are represented as means ± S.E. of five independent experiments, and the data shown in *D* are representative of three independent experiments with similar results. *WT*, wild type; *LA*, L1040A; *FA*, F1046A; *a.u.*, arbitrary unit.

knockdown studies, cells were transfected with siRNA using Lipofectamine RNAiMAX (Invitrogen) according to the forward transfection method of the manufacturer's instructions for 28 h, and then cells were transfected with pEGFP-C1 Daam1 CT. Cells were cultured in 0.5% fetal calf serum medium for 20 h and were processed for the fluorescence microscopy analysis and the immunoblotting analysis.

RESULTS

DAD Segment Reinforces the Actin Assembly Activity of the FH1-FH2 Domains of Daam1 in the Cytoplasmic Actin Assembly Assay—We previously established an *in vitro* cytoplasmic actin assembly assay to evaluate the actin assembly activity of FH1-FH2 domains of DRF in a cytoplasmic environment (11). Briefly, beads coated with recombinant carboxyl-terminal protein fragments of Daam1 (Daam1 CT) (Fig. 1*B*), which harbors FH1-FH2 domains and the DAD segment, are incubated with crude cytosol as a source of monomeric actin, and the assembled actin filaments on beads are quantified by rhodamine-phalloidin staining.

Using this assay, we attempted to characterize the contribution of DAD segment to the actin assembly activity of FH1-FH2 domains. The DAD segment contains several residues conserved among DRFs (Fig. 1*A*). We introduced a single amino acid substitution to Leu-1040 or Phe-1046 of Daam1 CT and examined the actin assembly activity of these mutants in the cytoplasmic actin assembly assay (Fig. 1*C*). The L1040A mutation diminished the actin assembly activity, whereas another mutant F1046A exhibited an actin assembly activity comparable with wild type.

Because the actin assembly in the cytoplasmic actin assembly assay requires the nucleation activity of formin CT protein (11), we tested the actin nucleation activity of Daam1 CT L1040A protein in the pyrene-actin assembly assay. Interestingly, the actin nucleation activity of Daam1 CT L1040A is indistinguishable from that of Daam1 CT WT or F1046A (Fig. 1*D*). Therefore, Daam1 L1040A mutant cannot assemble the actin filaments efficiently in the cytoplasmic environment, although it has the actin nucleation activity similar to that of the WT protein in the purified actin. These results suggest that some kind of cytosolic factor(s) may bind to Daam1 through the conserved leucine residue in the DAD segments and may assist Daam1 to assemble the actin filaments in the cytoplasmic environment.

Fli-I Interacts with the DAD Segment in the Carboxyl-terminal Region of Daam1—To identify this factor, we performed affinity chromatography with platelet cytosol using Daam1 CT WT and Daam1 CT L1040A as baits. GST-Daam1 CT WT- and GST-Daam1 CT L1040A-coated beads were incubated with platelet cytosol, and the bound proteins were analyzed by SDS-PAGE followed by Coomassie Brilliant Blue staining. By comparison of Daam1 CT WT-bound and Daam1 CT L1040A-bound proteins, a 145-kDa protein was specifically identified as a Daam1 CT WT-binding protein (Fig. 2*A*). MALDI-TOF MS analysis revealed that this protein was human Flightless-I homolog (Fli-I). This identification was confirmed by immunoblotting analysis with anti-Fli-I mAb. Fli-I was detected clearly in the eluate of Daam1 CT WT but faintly in the eluate of Daam1 CT L1040A (Fig. 2*B*). Fli-I is a conserved member of the gelsolin family. Fli-I was originally identified in *Drosophila* as a gene located in the locus that causes the degeneration of indirect flight muscle, which results in the "flightless" phenotype (19, 20). Fli-I-deficient nematode, fruit fly, and mouse exhibit the lethal phenotype in the very early embryonic development (21–23), which indicates that

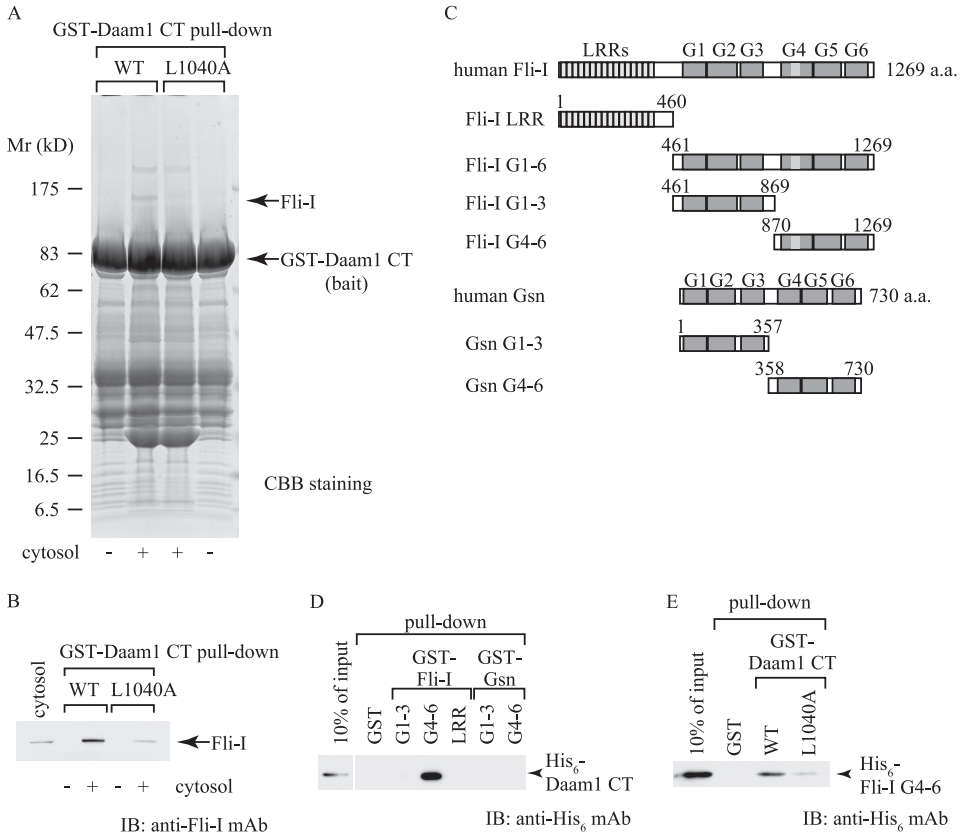

FIGURE 2. **Fli-I binds to DAD segment of Daam1.** *A* and *B*, Daam1 CT affinity chromatography. GST-Daam1 CT WT- or GST-Daam1 CT L1040A-coated beads were incubated with crude platelet cytosol or buffer alone, and the bound proteins were analyzed by Coomassie Brilliant Blue (*CBB*) staining (*A*) and immunoblot (*IB*) analysis using anti-Fli-I mAb (*B*). *C*, schematic representation of the domain structures of Fli-I and Gsn. *LRR*, leucine-rich repeat; *G1–6*, gelsolin motifs 1–6. *D*, direct binding of Daam1 to Fli-I. Beads coated with 50 pmol of GST, GST-Fli-I fragments, or GST-Gsn fragments were incubated with 62.5 nM His_6-Daam1 CT. Bead-bound proteins were analyzed by SDS-PAGE and immunoblotting. *E*, specific interaction of Daam1 and Fli-I. Beads coated with 12.5 pmol of GST-Daam1 CT were incubated with 2.5 μM His_6-Fli-I G4–6. Bead-bound proteins were analyzed by SDS-PAGE and immunoblotting. All the data shown in *D* and *E* are representative of three independent experiments with similar results.

Fli-I plays an essential role in the early developmental processes of metazoans.

Next, we attempted to determine the Daam1-binding region of Fli-I. Fli-I has 16 leucine-rich repeats at the amino terminus and 6 gelsolin motifs at the carboxyl terminus (Fig. 2*C*). We generated and purified several recombinant proteins corresponding to Fli-I fragments (Fig. 2*C*) and determined whether these fragments can bind to Daam1 CT *in vitro*. Fli-I G4–6 specifically interacted with Daam1 CT, whereas Fli-I LRR or Fli-I G1–3 did not bind to Daam1 CT (Fig. 2*D*). Because Fli-I belongs to the gelsolin family and the G4–6 region of Fli-I has 41% homology (18% identity) with the corresponding G4–6 region of Gsn (Fig. 2*C*), we evaluated whether Gsn can interact with Daam1. Neither Gsn G1–3 nor Gsn G4–6 bound to Daam1 CT (Fig. 2*D*). Furthermore, Daam1 CT L1040A mutant exhibited lower affinity for Fli-I G4–6 compared with the wild type proteins (Fig. 2*E*). These data indicate that Fli-I directly binds to the DAD segment of Daam1 through its G4–6 region.

Binding of Fli-I to the DAD Segment Enhances the Actin Assembly Activity of the FH1-FH2 Domains in Vitro—To evaluate whether Fli-I regulates the actin assembly activity of DRF, we first prepared cytosol from which Fli-I was completely immunodepleted (Fig. 3*A*). Then we examined the Daam1 CT-induced actin assembly in the Fli-I-depleted cytosol. Daam1 CT lost half of the actin assembly activity in the Fli-I-depleted cytosol compared with that of the control IgG-treated cytosol (Fig. 3*C*). The addition of recombinant Fli-I (Fig. 3*B*) restored the Daam1 CT-induced actin assembly in Fli-I-depleted cytosol (Fig. 3*C*). These results indicate that Fli-I enhances the Daam1 CT-induced actin assembly.

Fli-I Is Required for the Daam1 CT-induced Actin Assembly in Living Cells—Next, we evaluated whether Fli-I is involved in the formin-induced actin assembly in living cells. It has been reported that the exogenous expression of Daam1 CT induces a stress fiber formation in HeLa cells (24). The overexpression of GFP-tagged Daam1 CT WT induced the formation of stress fiber-like filaments in serum-starved NIH 3T3 cells, whereas GFP alone did not (Fig. 4, *A* and *B*). In GFP-Daam1 CT L1040A-expressing cells, such stress fiber formation was scarcely induced compared with Daam1 CT WT (Fig. 4, *A* and *B*), which suggests that the Fli-I binding is required for Daam1 CT to exert its actin assembly activity in cells.

We further examined the significance of Fli-I using a gene knock-down technique. Transfection of two different siRNAs against Fli-I (#1 and #2) almost completely reduced the Fli-I expression level in NIH 3T3 cells (Fig. 5*A*). Daam1 CT-induced stress fiber formation was significantly reduced in the Fli-I siRNA #1- and #2-treated cells but not in the control siRNA-treated cells (Fig. 5*B*). Co-expression of siRNA-insensitive human Fli-I with Daam1 CT restored the stress fiber formation in the Fli-I knocked down cells (Fig. 5, *A* and *B*). The co-expression of Fli-I and GFP alone did not induce the actin stress fiber formation in the NIH 3T3 cells (supplemental Fig. 2). These results demonstrate that Fli-I is essential for Daam1 FH1-FH2 domains to assemble actin filaments in living cells.

Fli-I Facilitates the Rho-induced Activation of Daam1—Although the activation of DRF is mediated by the binding of GTP-bound active Rho to the GBD domain, GTP-RhoA binding alone is insufficient for the full recovery of the actin assembly activity of DRF CT in the presence of DRF NT *in vitro* (12, 15). Therefore, some additional factor(s) other than GTP-Rho is (are) supposed to be required for full DRF activation (1, 2, 12, 15, 25). It has been proposed that the activation of DRF is specifically mediated by the dissociation of the DID domain from the DAD segment. Because Fli-I binds to DRF through the DAD segment, it is conceivable

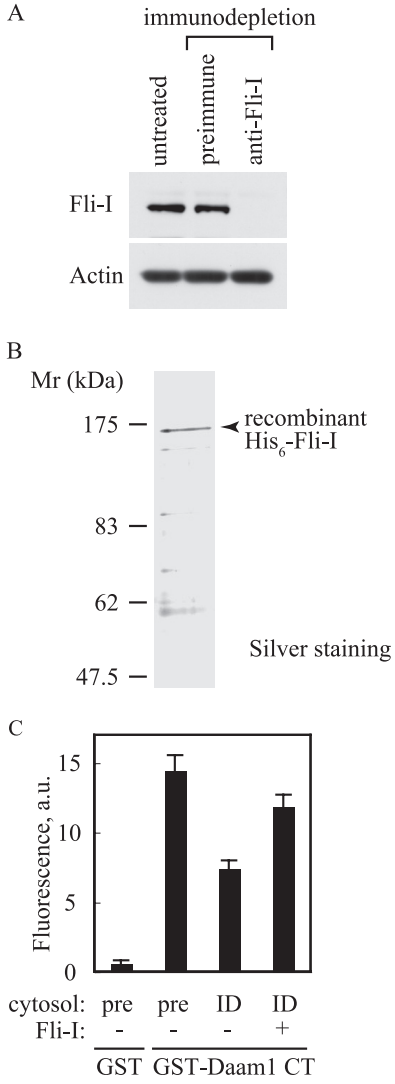

FIGURE 3. **Fli-I enhances the actin assembly activity of Daam1 CT in the cytoplasmic environment.** *A,* immunodepletion of Fli-I. Human platelet cytosol was incubated with preimmune IgG- or anti-Fli-I IgG-coated beads. After centrifugation, the supernatant was analyzed by SDS-PAGE and immunoblotting with anti-Fli-I mAb and anti-actin mAb. Actin was used as a loading control. *B,* purified recombinant His_6-tagged Fli-I was analyzed by SDS-PAGE followed by silver staining. *C,* cytoplasmic actin assembly was measured for 10 pmol of Daam1 CT in Fli-I-depleted cytosol in the absence or presence of 125 nM purified Fli-I. *pre*, preimmune IgG-treated cytosol; *ID*, Fli-I-immunodepleted cytosol. The data shown are represented as means ± S.E. of five independent experiments. *a.u.,* arbitrary unit.

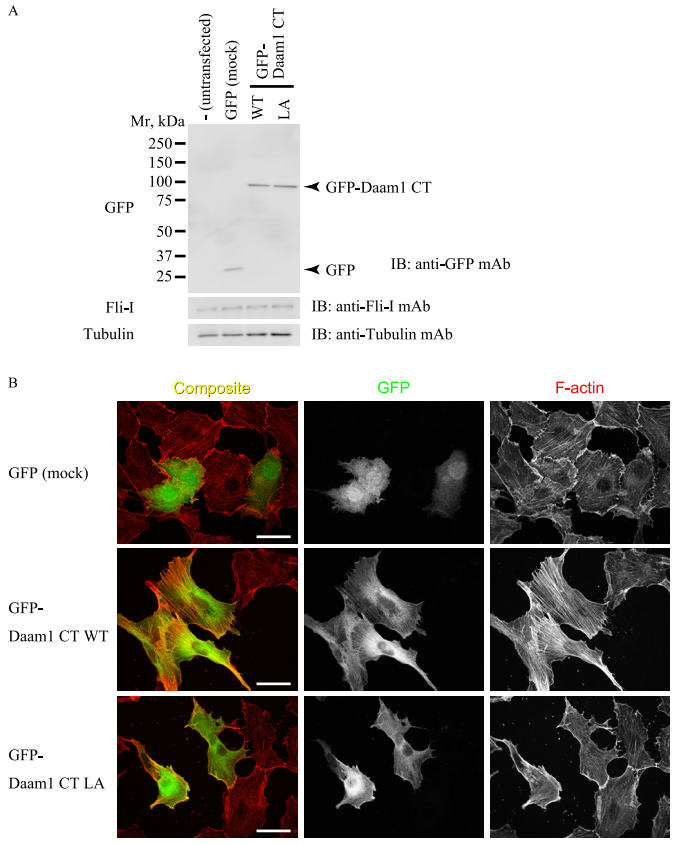

FIGURE 4. **DAD segment of Daam1 enhances the actin assembly in living cells.** *A* and *B,* NIH 3T3 cells were transiently transfected with GFP-Daam1 CT WT, GFP-Daam1 CT L1040A, or control GFP vector. After 20 h, the cell lysates were analyzed by SDS-PAGE and immunoblotting (*IB*) with anti-GFP, anti-Fli-I, and anti-tubulin mAbs (*A*), and cells were stained with Alexa-568-phalloidin (*red*). GFP signals were shown in *green*. *WT,* wild type; *LA*, L1040A. *Scale bars*, 20 μm (*B*). The data shown are representative of at least three independent experiments with similar results.

that Fli-I is involved in the relief of DID-DAD autoinhibitory interaction by Rho GTPase.

To evaluate this possibility, we first examined whether Fli-I competes with the DID domain in the DAD segment binding. Daam1 NT containing the DID domain inhibited the binding of Fli-I to Daam1 DAD in a concentration-dependent manner (Fig. 6*A*). These results indicate that Fli-I and the DID domain cannot bind to the DAD segment simultaneously.

Although RhoA G14V, a GTP-bound state-locked mutant, alone could dissociate Daam1 NT from Daam1 DAD, the full disruption of the DID-DAD interaction required high concentrations (2.5 μM) of RhoA G14V *in vitro* (Fig. 6*B*). In the presence of RhoA G14V at low concentrations (0.1 and 0.5 μM), we detected only slight disruption of DID-DAD interaction (Fig. 6*B*). However, the addition of Fli-I concentration-dependently promoted the dissociation of Daam1 NT from Daam1 DAD in the presence of 0.1 μM RhoA G14V (Fig. 6*C*). Because Fli-I alone hardly displaced Daam1 NT from Daam1 DAD segment (Fig. 6*C*), the stimulatory effect of Fli-I on the DID-DAD dissociation is dependent on the presence of GTP-Rho.

Next, we evaluated whether Fli-I actually facilitates GTP-Rho-mediated actin assembly by DRFs. In the pyrene-actin assembly assay, Daam1 CT nucleated actin assembly (Fig. 6*D*). This activity was almost totally inhibited by the addition of Daam1 NT, and the inhibition was partially relieved by the addition of GTP-RhoA, as shown previously (12, 15). The addition of Fli-I G4–6 together with RhoA G14V resulted in increased liberation of the actin assembly activity of Daam1 CT suppressed by Daam1 NT (Fig. 6*D*), whereas Fli-I G4–6 alone had no actin assembly activity. Thus, Fli-I serves as a stimulatory factor of Rho-mediated activation of DRFs.

Fli-I Is a Common Positive Regulator for Daam1 and mDia1—Finally, we evaluated whether the regulatory mechanism of Daam1 by Fli-I is conserved in other DRFs. mDia1 is closely related to Daam1 and has a domain structure similar to that of Daam1 (Fig. 1*B*). We generated a carboxyl-terminal fragment protein of mDia1 (mDia1 CT) harboring L1197A mutation, which corresponds to L1040A mutation in Daam1, and we eval-

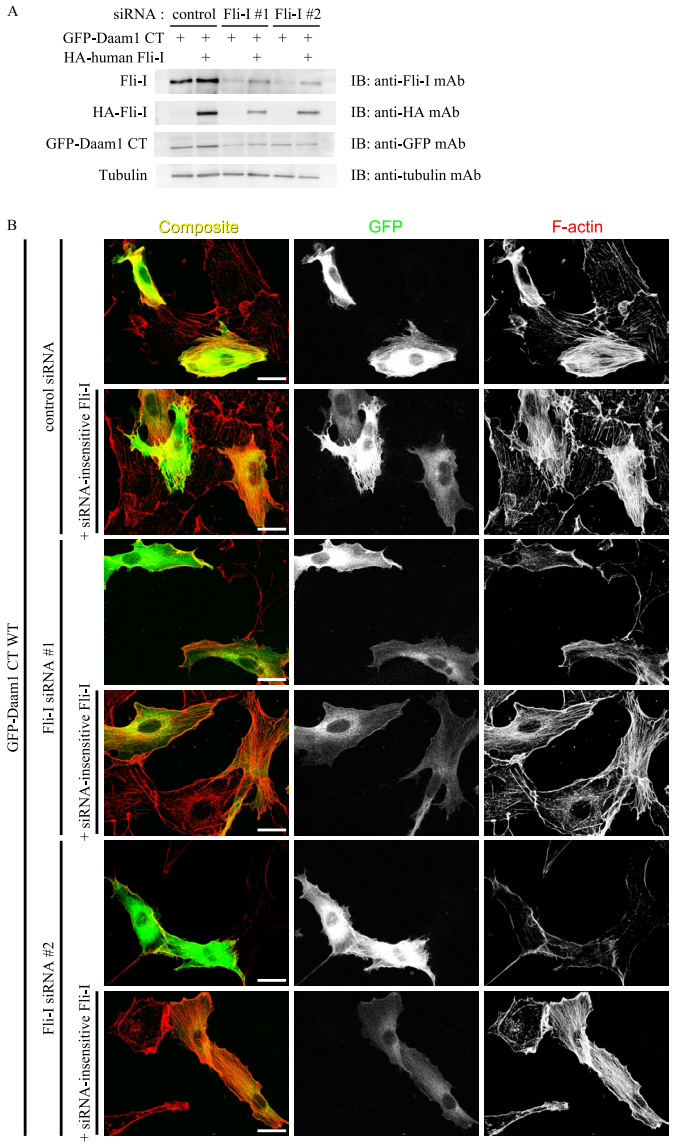

FIGURE 5. **Fli-I is required for the actin assembly by Daam1 in living cells.** *A* and *B*, NIH 3T3 cells were transfected with control or Fli-I siRNA. After 28 h, the cells were transiently transfected with GFP-Daam1 CT and/or hemagglutinin-tagged siRNA-insensitive Fli-I. After 20 h, cells were analyzed by SDS-PAGE and immunoblotting with anti-Fli-I, anti-GFP, anti-hemagglutinin, and anti-tubulin mAbs (*A*) or were stained with Alexa-568-phalloidin (*red*). GFP signals are shown in *green*. *B, scale bars*, 20 μm. The data shown are representative of at least three independent experiments with similar results.

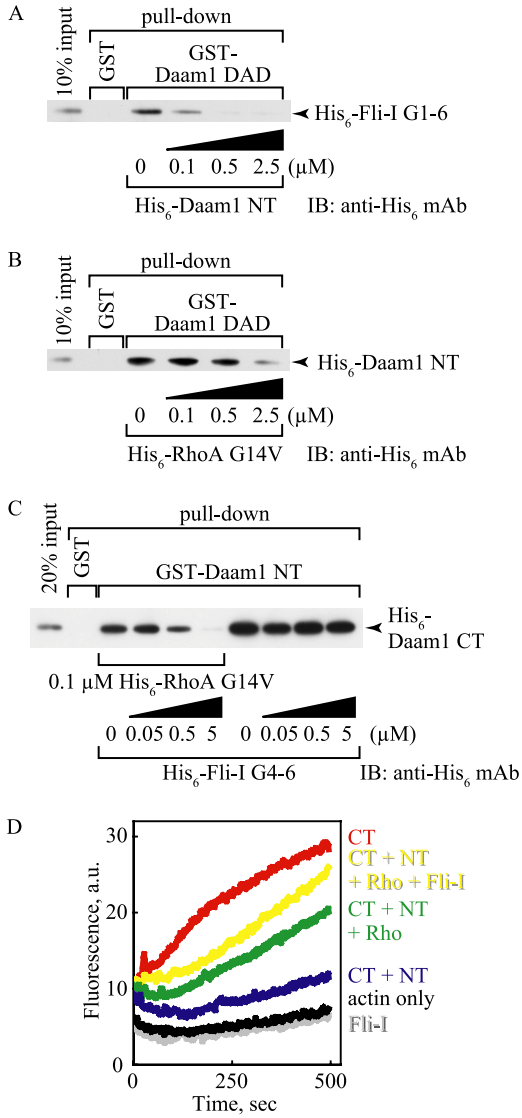

FIGURE 6. **Fli-I enhances the GTP-RhoA-mediated dissociation of the DID domain from the DAD segment.** *A*, Fli-I competes with the DID domain on DAD binding. 50 pmol of GST-Daam1 DAD-coated beads were incubated with 25 pmol of His_6-Fli-I G1–6 in the presence of various concentrations of His_6-Daam1 NT. Bead-associated His_6-Fli-I G1–6 was detected by immunoblotting (*IB*). *B*, concentration-dependent disruption of DID-DAD interaction by GTP-RhoA. Beads coated with 50 pmol of GST-Daam1 DAD were incubated with 125 nM His_6-Daam1 NT in the presence of various concentrations of His_6-RhoA G14V. Bead-associated His_6-Daam1 NT was analyzed by immunoblotting with anti-His_6 mAb. *C*, Fli-I enhances the DID-DAD dissociation of Daam1 by GTP-RhoA. Beads coated with 20 pmol of GST-Daam1 NT were incubated with 100 nM His_6-Daam1 CT in the absence or presence of 0.1 μM His_6-RhoA G14V and various concentrations of His_6-Fli-I G4–6. Bead-bound His_6-Daam1 CT was detected by immunoblotting. *D*, Fli-I promotes the Daam1 activation by GTP-RhoA. The actin nucleation activity of 50 nM Daam1 CT in the absence or presence of 200 nM Daam1 NT, 800 nM Fli-I G4–6, and 250 nM RhoA G14V was evaluated by the pyrene-actin assembly assay, as indicated. *a.u.*, arbitrary unit. All the data shown in *A–D* are representative of 3–5 independent experiments with similar results.

uated its actin assembly activity in the cytoplasmic actin assembly assay. mDia1 L1197A exhibited reduced actin assembly activity compared with mDia1 CT WT or F1203A, which corresponds to F1046A in Daam1 (Fig. 7*A*). The actin nucleation activity of mDia1 CT L1197A was comparable with mDia1 CT WT or F1203A in the pyrene-actin assembly assay (supplemental Fig. 1*A*). mDia1 CT interacted directly with Fli-I G4–6 region (Fig. 7*B*) dependent on the Leu-1197 residue (supplemental Fig. 1*B*). The immunodepletion of Fli-I from the cytosol reduced the actin assembly activity of mDia1 CT in the cytoplasmic actin assembly assay, and the activity was rescued by the addition of recombinant Fli-I (Fig. 7*C*). As observed for Daam1, mDia1 NT competes with Fli-I on the binding to mDia1 DAD (supplemental Fig. 1*C*). Although a relatively higher concentration of RhoA G14V (0.5 μM) was required for the disruption of the DID-DAD interaction of mDia1 in the absence of Fli-I (Fig. 7*D*), a lower concentration of RhoA G14V (0.1 μM) induced the DID-DAD dissociation in the presence of Fli-I (Fig. 7*E*). Finally, the addition of Fli-I G4–6 enhanced the Rho-mediated activation of the actin nucleation activity of mDia1 CT in the presence of mDia1 NT in the pyrene-actin

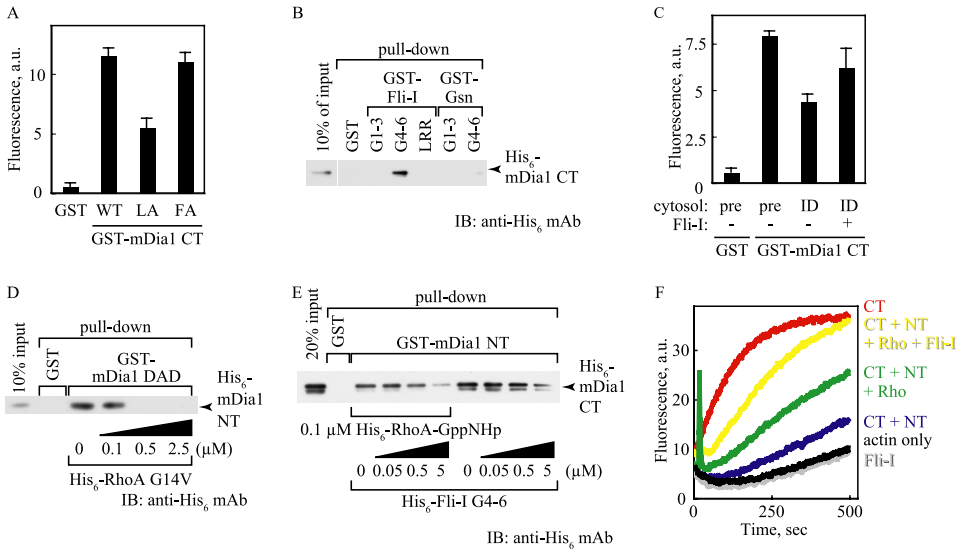

FIGURE 7. **Fli-I enhances the actin assembly activity of mDia1 as well as that of Daam1.** *A*, cytoplasmic actin assembly assay of mDia1 CT mutants. *WT*, wild type; *LA*, L1197A; *FA*, F1203A. *B*, direct binding of mDia1 to Fli-I. Beads coated with 50 pmol of GST-tagged proteins were incubated with 12.5 pmol of His_6-tagged proteins as indicated. Bound proteins were analyzed by SDS-PAGE and immunoblotting (*IB*). *C*, cytoplasmic actin assembly was measured for 1 pmol of mDia1 CT in Fli-I-depleted cytosol used in Fig. 3*C* in the absence or presence of 125 nM purified Fli-I. *pre*, preimmune IgG-treated cytosol; *ID*, Fli-I-immunodepleted cytosol. *D*, concentration-dependent disruption of DID-DAD interaction of mDia1 by GTP-RhoA. Beads coated with 50 pmol of GST-mDia1 DAD were incubated with 125 nM His_6-mDia1 NT in the presence of various concentrations of His_6-RhoA G14V. Bead-associated His_6-mDia1 NT was analyzed by immunoblotting with anti-His_6 mAb. *E*, Fli-I enhances the DID-DAD dissociation of mDia1 by GTP-RhoA. Beads coated with 100 nM GST-mDia1 NT were incubated with 20 pmol of His_6-mDia1 CT in the absence or presence of 0.1 μM His_6-RhoA G14V and various concentrations of His_6-Fli-I G4–6. Bead-bound His_6-mDia1 CT was detected by immunoblotting. *F*, Fli-I promotes the mDia1 activation by GTP-RhoA. The actin nucleation activity of 5 nM mDia1 CT in the absence or presence of 20 nM mDia1 NT, 400 nM Fli-I G4–6, and 100 nM RhoA G14V was evaluated by the pyrene-actin assembly assay, as indicated. The data shown in *A* and *C* are represented as means ± S.E. of five independent experiments, and the data shown in *B* and *D–F* are representative of three independent experiments with similar results. *a.u.*, arbitrary unit.

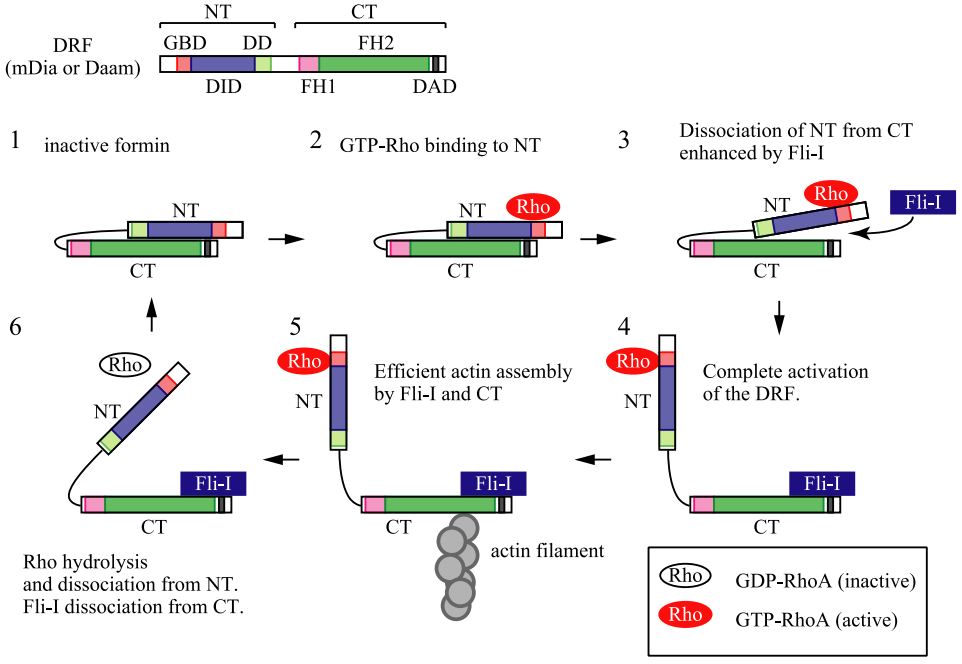

FIGURE 8. **Model for the regulation of DRF-mediated actin assembly by Rho and Fli-I.** See text for details.

assembly assay (Fig. 7*F*). These results suggest that Fli-I binds to mDia1 through the G4–6 region and that Fli-I assists GTP-Rho to release the actin assembly activity of mDia1 by disrupting the autoinhibitory interaction of mDia1. Thus, Fli-I is a common regulator of two DRF members, Daam1 and mDia1.

DISCUSSION

Here, we identified Fli-I as a DRF (Daam1 or mDia1)-binding protein. We then demonstrated that Fli-I has dual functions on the DRF-mediated actin assembly as follows: 1) to assist GTP-Rho to activate DRFs by disrupting the inhibitory interaction between DID and DAD, and 2) to elevate the actin assembly activity of DRF FH1-FH2 domains regardless of DRF regulation by GTP-Rho.

Based on the results presented here, we propose a model for the regulatory mechanism of DRF-mediated actin assembly as follows (Fig. 8). 1) Without GTP-Rho, DRF is kept inactive by the intramolecular DID-DAD interaction. 2) Upon binding of GTP-Rho to the GBD domain, the DID-DAD interaction becomes partially perturbed. 3) Subsequent Fli-I binding to the DAD segment competitively accelerates the dissociation of the DID domain from the DAD segment. 4) The disruption of DID-DAD interaction results in the exposure of the FH1-FH2 domains. 5) The FH1-FH2 domains assemble the actin filaments in cooperation with Fli-I bound to the DAD segment. 6) When Rho is inactivated by GTP hydrolysis, GDP-Rho dissociates from the GBD domain, and Fli-I is released from the DAD segment, which leads to inactivation of DRF by reassociation of the DID domain and the DAD segment. For simplicity, the DRF is shown as a monomer in Fig. 8, although DRF is thought to form dimer or multimer.

It was believed that a putative factor is required for the GTP-Rho-mediated full activation of DRF (1, 2, 12, 15, 25). In our previous study, we showed that GTP-RhoA, -B, and -C can fully relieve the autoinhibition of Daam1 and mDia1 in the cytoplasmic environment using the cytoplasmic actin assembly assay (11), which suggested that the cytosol contains the putative factor required for the full activation of DRF. In this study, we demonstrated that the cyto-

solic factor Fli-I displaces the DID domain from the DAD segment in the presence of GTP-Rho. Displacement of the DID domain from the DAD segment leads to the assembly of actin by FH1-FH2 domains. Taken together, Fli-I is likely to be the putative missing factor for the Rho-mediated activation of DRFs.

Fli-I not only enhances the DID-DAD dissociation, but also reinforces the actin assembly activity of the FH1-FH2 domain (Fig. 1*C*, Fig. 3*C*, Fig. 4, and Fig. 7, *A* and *C*). Because Fli-I can bind both globular actin and F-actin (26), Fli-I would support the actin assembly activity of DRF by holding the preformed F-actin or by recruiting globular actin. In the budding yeast, a formin protein Bni1p assembles the actin cables and promotes cytokinesis (5, 27–29), where an actin-interacting protein Bud6p binds to Bni1p through the region adjacent to DAD, and promotes the Bni1p-mediated actin assembly (8, 25, 30). Because the metazoan genomes do not contain a Bud6p homolog, Fli-I could be functionally equivalent to Bud6p in metazoans, although they share no homology in their primary structures (8, 25).

Because the Fli-I-binding sequence is conserved in human Daam1, Daam2, mDia1, mDia2, and mDia3, *Drosophila* Daam and Diaphanous, and *Caenorhabditis elegans* Daam (F56E10.2) (Fig. 1*A*), the regulatory mechanism of these DRFs by Fli-I is probably conserved throughout the metazoan evolution. Indeed, the loss of either Fli-I or Diaphanous in *Drosophila* caused similar defects in actin distribution during the cellularization process (23, 31), which suggests that Diaphanous and Fli-I function cooperatively in the early developmental stage of *Drosophila*.

Despite the importance of Daam proteins in development, the molecular mechanisms involved in Daam proteins have not been well understood (32). Daam1 was originally identified as a binding protein of Dishevelled, a Frizzled (Wnt receptor)-binding protein (24), and Daam1 binding to Dishevelled activates Rho through its putative guanine nucleotide exchange factor, which results in the signal transduction of planar cell polarity (PCP) pathway in *Xenopus* (24, 33). On the other hand, in *Drosophila*, *DAAM* interacts genetically with *Rho1* (34), and loss-of-function analysis of DAAM in the wing and compound eye, which are conventional PCP organization model tissues, revealed that DAAM is not involved in the PCP signaling (34). Our previous study (11) and present results show that Daam1 as well as mDia1 are the direct Rho effector molecules, which mediate the actin assembly using Fli-I as a common cofactor. Taken together, vertebrate Daam1 might be a dual functional protein that is a PCP regulator and a Rho effector, whereas the *Drosophila* DAAM is principally a Rho effector. Further analysis of the relationship of Rho and Daam in the vertebrate PCP signaling would be necessary.

In summary, we have demonstrated that Fli-I helps GTP-Rho to activate the FH1-FH2-mediated actin assembly by competitively promoting the disruption of the inhibitory interaction between the DID domain and DAD segment of DRFs. Furthermore, Fli-I enhances the actin assembly activity of DRF *in vitro* and in living cells through direct binding to the DAD segment of DRF. Therefore, Fli-I is an important co-factor for the mammalian formin proteins, Daam1 and mDia1.

Acknowledgments—We are grateful to the Kyoto Red Cross Blood Center for providing platelet pellets. We thank Tomoko Matsubara for excellent technical assistance.

REFERENCES

1. Faix, J., and Grosse, R. (2006) *Dev. Cell* **10,** 693–706
2. Higgs, H. N. (2005) *Trends Biochem. Sci.* **30,** 342–353
3. Paul, A. S., and Pollard, T. D. (2009) *Cell Motil. Cytoskeleton* **66,** 606–617
4. Pruyne, D., Evangelista, M., Yang, C., Bi, E., Zigmond, S., Bretscher, A., and Boone, C. (2002) *Science* **297,** 612–615
5. Sagot, I., Rodal, A. A., Moseley, J., Goode, B. L., and Pellman, D. (2002) *Nat. Cell Biol.* **4,** 626–631
6. Westendorf, J. J., Mernaugh, R., and Hiebert, S. W. (1999) *Gene* **232,** 173–182
7. Yamashita, M., Higashi, T., Suetsugu, S., Sato, Y., Ikeda, T., Shirakawa, R., Kita, T., Takenawa, T., Horiuchi, H., Fukai, S., and Nureki, O. (2007) *Genes Cells* **12,** 1255–1265
8. Moseley, J. B., Sagot, I., Manning, A. L., Xu, Y., Eck, M. J., Pellman, D., and Goode, B. L. (2004) *Mol. Biol. Cell* **15,** 896–907
9. Kovar, D. R., Kuhn, J. R., Tichy, A. L., and Pollard, T. D. (2003) *J. Cell Biol.* **161,** 875–887
10. Alberts, A. S. (2002) *Curr. Biol.* **12,** R796
11. Higashi, T., Ikeda, T., Shirakawa, R., Kondo, H., Kawato, M., Horiguchi, M., Okuda, T., Okawa, K., Fukai, S., Nureki, O., Kita, T., and Horiuchi, H. (2008) *J. Biol. Chem.* **283,** 8746–8755
12. Li, F., and Higgs, H. N. (2003) *Curr. Biol.* **13,** 1335–1340
13. Alberts, A. S. (2001) *J. Biol. Chem.* **276,** 2824–2830
14. Watanabe, N., Kato, T., Fujita, A., Ishizaki, T., and Narumiya, S. (1999) *Nat. Cell Biol.* **1,** 136–143
15. Li, F., and Higgs, H. N. (2005) *J. Biol. Chem.* **280,** 6986–6992
16. Christoforidis, S., McBride, H. M., Burgoyne, R. D., and Zerial, M. (1999) *Nature* **397,** 621–625
17. Laemmli, U. K. (1970) *Nature* **227,** 680–685
18. Kawato, M., Shirakawa, R., Kondo, H., Higashi, T., Ikeda, T., Okawa, K., Fukai, S., Nureki, O., Kita, T., and Horiuchi, H. (2008) *J. Biol. Chem.* **283,** 166–174
19. Campbell, H. D., Schimansky, T., Claudianos, C., Ozsarac, N., Kasprzak, A. B., Cotsell, J. N., Young, I. G., de Couet, H. G., and Miklos, G. L. (1993) *Proc. Natl. Acad. Sci. U.S.A.* **90,** 11386–11390
20. Perrimon, N., Smouse, D., and Miklos, G. L. (1989) *Genetics* **121,** 313–331
21. Deng, H., Xia, D., Fang, B., and Zhang, H. (2007) *Genetics* **177,** 847–860
22. Campbell, H. D., Fountain, S., McLennan, I. S., Berven, L. A., Crouch, M. F., Davy, D. A., Hooper, J. A., Waterford, K., Chen, K. S., Lupski, J. R., Ledermann, B., Young, I. G., and Matthaei, K. I. (2002) *Mol. Cell. Biol.* **22,** 3518–3526
23. Straub, K. L., Stella, M. C., and Leptin, M. (1996) *J. Cell Sci.* **109,** 263–270
24. Habas, R., Kato, Y., and He, X. (2001) *Cell* **107,** 843–854
25. Goode, B. L., and Eck, M. J. (2007) *Annu. Rev. Biochem.* **76,** 593–627
26. Goshima, M., Kariya, K., Yamawaki-Kataoka, Y., Okada, T., Shibatohge, M., Shima, F., Fujimoto, E., and Kataoka, T. (1999) *Biochem. Biophys. Res. Commun.* **257,** 111–116
27. Ozaki-Kuroda, K., Yamamoto, Y., Nohara, H., Kinoshita, M., Fujiwara, T., Irie, K., and Takai, Y. (2001) *Mol. Cell. Biol.* **21,** 827–839
28. Imamura, H., Tanaka, K., Hihara, T., Umikawa, M., Kamei, T., Takahashi, K., Sasaki, T., and Takai, Y. (1997) *EMBO J.* **16,** 2745–2755
29. Kohno, H., Tanaka, K., Mino, A., Umikawa, M., Imamura, H., Fujiwara, T., Fujita, Y., Hotta, K., Qadota, H., Watanabe, T., Ohya, Y., and Takai, Y. (1996) *EMBO J.* **15,** 6060–6068
30. Moseley, J. B., and Goode, B. L. (2005) *J. Biol. Chem.* **280,** 28023–28033
31. Afshar, K., Stuart, B., and Wasserman, S. A. (2000) *Development* **127,** 1887–1897
32. Liu, R., Linardopoulou, E. V., Osborn, G. E., and Parkhurst, S. M. (2010) *Biochim. Biophys. Acta* **1803,** 207–225
33. Liu, W., Sato, A., Khadka, D., Bharti, R., Diaz, H., Runnels, L. W., and Habas, R. (2008) *Proc. Natl. Acad. Sci. U.S.A.* **105,** 210–215
34. Matusek, T., Djiane, A., Jankovics, F., Brunner, D., Mlodzik, M., and Mihály, J. (2006) *Development* **133,** 957–966